



**HAL**  
open science

## **Running Head: nutrient enrichment on a coral reef Landscape-scale patterns of nutrient enrichment in a coral reef ecosystem: implications for coral to algae phase shifts**

Thomas C Adam, Deron E Burkepile, Sally J Holbrook, Robert C Carpenter,  
Joachim Claudet, Charles Loiseau, Lauric Thiault, Andrew J Brooks, Libe  
Washburn, Russell J Schmitt

### ► **To cite this version:**

Thomas C Adam, Deron E Burkepile, Sally J Holbrook, Robert C Carpenter, Joachim Claudet, et al..  
Running Head: nutrient enrichment on a coral reef Landscape-scale patterns of nutrient enrichment  
in a coral reef ecosystem: implications for coral to algae phase shifts. *Ecological Applications*, 2021,  
31 (1), pp.e2227. 10.1002/eap.2227 . hal-03107510

**HAL Id: hal-03107510**

**<https://hal.science/hal-03107510v1>**

Submitted on 12 Jan 2021

**HAL** is a multi-disciplinary open access archive for the deposit and dissemination of scientific research documents, whether they are published or not. The documents may come from teaching and research institutions in France or abroad, or from public or private research centers.

L'archive ouverte pluridisciplinaire **HAL**, est destinée au dépôt et à la diffusion de documents scientifiques de niveau recherche, publiés ou non, émanant des établissements d'enseignement et de recherche français ou étrangers, des laboratoires publics ou privés.

1 Running Head: nutrient enrichment on a coral reef

2 **Landscape-scale patterns of nutrient enrichment in a coral reef ecosystem: implications for**  
3 **coral to algae phase shifts**

4 Thomas C. Adam<sup>1\*</sup>, Deron E. Burkepile<sup>1,2</sup>, Sally J. Holbrook<sup>1,2</sup>, Robert C. Carpenter<sup>3</sup>, Joachim  
5 Claudet<sup>4,5</sup>, Charles Loiseau<sup>4,5</sup>, Lauric Thiault<sup>4,5</sup>, Andrew J. Brooks<sup>1</sup>, Libe Washburn<sup>1,6</sup>, Russell J.  
6 Schmitt<sup>1,2</sup>

7 <sup>1</sup>Marine Science Institute, University of California, Santa Barbara, California 93106, USA

8 <sup>2</sup>Department of Ecology, Evolution, and Marine Biology, University of California, Santa  
9 Barbara, California 93106, USA

10 <sup>3</sup>Department of Biology, California State University Northridge, Northridge, California 91330

11 <sup>4</sup>National Center for Scientific Research, PSL Université Paris, CRIOBE, USR 3278 CNRS-  
12 EPHE-UPVD, Maison des Océans, 195 rue Saint-Jacques 75005 Paris, France

13 <sup>5</sup>Laboratoire d'Excellence CORAIL, Moorea, French Polynesia

14 <sup>6</sup>Department of Geography, University of California, Santa Barbara, California 93106, USA

15

16 \*corresponding author: thomascadam@gmail.com

17

18 **Abstract**

19           Nutrient pollution is altering coastal ecosystems worldwide. On coral reefs, excess  
20 nutrients can favor the production of algae at the expense of reef-building corals, yet the role of  
21 nutrients in driving community changes such as shifts from coral to macroalgae is not well  
22 understood. Here we investigate the potential role of anthropogenic nutrient loading in driving  
23 recent coral-to-macroalgae phase shifts on reefs in the lagoons surrounding the Pacific island of  
24 Moorea, French Polynesia. We use nitrogen (N) tissue content and stable isotopes ( $\delta^{15}\text{N}$ ) in an  
25 abundant macroalga (*Turbinaria ornata*) together with empirical models of nutrient discharge to  
26 describe spatial and temporal patterns of nutrient enrichment in the lagoons. We then employ  
27 time series data to test whether recent increases in macroalgae are associated with nutrients. Our  
28 results revealed that patterns of N enrichment were linked to several factors, including rainfall,  
29 wave-driven circulation, and distance from anthropogenic nutrient sources, especially human  
30 sewage. Reefs near large watersheds, where inputs of N from sewage and agriculture are high,  
31 have been consistently enriched in N for at least the last decade. In many of these areas, corals  
32 have decreased and macroalgae have increased, while reefs with lower levels of N input have  
33 maintained high cover of coral and low cover of macroalgae. Importantly, these patchy phase  
34 shifts to macroalgae have occurred despite substantial island-wide increases in the density and  
35 biomass of herbivorous fishes over the time period. Together, these results indicate that nutrient  
36 loading may be an important driver of coral-to-macroalgae phase shifts in the lagoons of Moorea  
37 even though the reefs harbor an abundant and diverse herbivore assemblage. These results  
38 emphasize the important role that bottom-up factors can play in driving coral-to-macroalgae  
39 phase shifts and underscore the critical importance of watershed management for reducing inputs  
40 of nutrients and other land-based pollutants to coral reef ecosystems.

41 **Key words:** *coral reef; phase shift; macroalgae; nutrient pollution; nitrogen; sewage; top-*  
42 *down; bottom-up; Turbinaria ornata; stable isotopes;  $\delta^{15}N$ ; herbivory*

### 43 **Introduction**

44 Nutrient pollution is a major anthropogenic force altering coastal ecosystems worldwide  
45 (Carpenter et al. 1998, Howarth 2008). Anthropogenic inputs of nitrogen and phosphorous can  
46 facilitate blooms of harmful algae, reduce water clarity, alter food webs, and deplete oxygen  
47 leading to dead zones (Boesch 2002), ultimately disrupting fisheries and harming human health  
48 (Anderson et al. 2012). These adverse effects of excess nutrients on coastal ecosystems are likely  
49 to be exacerbated in coming decades by continued changes in land-use as well as altered  
50 precipitation regimes and ocean warming due to climate change (Altieri and Gedan 2015, Gobler  
51 et al. 2017, Sinha et al. 2017).

52 Excess nutrients can be especially harmful to oligotrophic systems such as coral reefs.  
53 High levels of nutrient loading can lead to persistent blooms of algae that can dramatically alter  
54 the structure and function of reef ecosystems (Naim 1993, Loya 2004, Lapointe et al. 2005).  
55 Even moderate nutrient loading can favor algae and heterotrophic filter feeders that compete  
56 with corals and other reef building taxa (Fabricius 2005, Rice et al. 2020), thereby impeding  
57 coral recovery following a disturbance (Graham et al. 2015, MacNeil et al. 2019). Nitrogen (N)  
58 loading can be particularly harmful to coral reefs, as excess N can negatively impact coral  
59 growth and survival in addition to fueling algal growth (D'Angelo and Wiedenmann 2014,  
60 Shantz and Burkepile 2014, Morris et al. 2019). Thus, understanding the sources and impacts of  
61 anthropogenic N is critical for conservation and management of coral reef ecosystems.

62           In some cases, N pollution can be traced to a specific point source (e.g., sewage outfall)  
63 (Smith et al. 1981, Dailer et al. 2010). However, most N input to coastal ecosystems is derived  
64 from diffuse nonpoint sources (Carpenter et al. 1998). On coral reefs, N from nonpoint sources  
65 tends to be delivered in surface water runoff during episodic rainfall events and via discharge of  
66 submarine groundwater. After reaching the ocean, N-rich water is then transported and mixed via  
67 local hydrodynamic features. Small-scale hydrodynamics also influence rates of nutrient uptake  
68 by modifying boundary-layer conditions of benthic organisms (Carpenter et al. 1991). Thus, the  
69 movement and ultimate fate of anthropogenically-derived N in nearshore ecosystems are  
70 complex and will depend on many interacting factors, including the location of N sources, the  
71 timing of rainfall, and the hydrodynamic environment (Brocke et al. 2015).

72           A more complete understanding of the impacts of N pollution on nearshore ecosystems  
73 requires knowledge of the spatial and temporal patterns of enrichment and how the physical  
74 environment modulates these patterns. In many locations, water column nutrients are measured  
75 periodically in mandated water quality monitoring programs. These programs can provide  
76 valuable information on decadal-scale trends and large-scale spatial patterns of nutrient  
77 availability (De’Ath and Fabricius 2010, Duprey et al. 2016, Lapointe et al. 2019). However, the  
78 coarse temporal and spatial resolution of most water column monitoring programs precludes  
79 building a mechanistic understanding of the causes and consequences of nutrient enrichment in  
80 many coastal systems. This is particularly true on coral reefs, where researchers have used N  
81 content and isotopic signatures in benthic algae to resolve patterns of N enrichment at relatively  
82 small spatial scales (Umezawa et al. 2002, Lin and Fong 2008, Dailer et al. 2010). However,  
83 these studies generally have not linked enrichment patterns to benthic community dynamics or  
84 ecosystem processes (but see Lapointe 1997). As a result, there is widespread disagreement

85 regarding the levels of nutrient enrichment that are harmful to coral reefs and how important  
86 nutrients are for impacting coral reef community dynamics (Lapointe 1999, Szmant 2002,  
87 D'Angelo and Wiedenmann 2014, Arias-González et al. 2017, Bruno et al. 2019).

88 Here we quantify the spatial and temporal patterns of N availability on coral reefs around  
89 the South Pacific island of Moorea, French Polynesia. The coral reefs around Moorea have  
90 undergone multiple cycles of disturbance and recovery over the past four decades. While the  
91 oligotrophic fore reef has shown remarkable resilience to disturbances (Adjeroud et al. 2009,  
92 2018, Holbrook et al. 2018, Kayal et al. 2018), the reefs within the lagoons have exhibited  
93 contrasting dynamics, with some reefs shifting from coral- to macroalgae-dominated  
94 communities (Schmitt et al. 2019). Nutrient input could be a major driver of algal proliferation  
95 within the lagoons, but to date, no studies have evaluated the spatial or temporal patterns of  
96 enrichment or how those patterns relate to benthic community dynamics. Here, we combine N  
97 content and stable isotopes ( $\delta^{15}\text{N}$ ) in the tissue of the macroalga *Turbinaria ornata*, together with  
98 empirical models of nutrient discharge and time series data on the dynamics of benthic algae and  
99 coral to address the following questions: 1) What are the spatial patterns of N enrichment and  
100 how do these patterns vary across seasons with different levels of rainfall and wave forcing? 2)  
101 To what extent are spatial patterns of N enrichment related to anthropogenic inputs? and 3) Are  
102 recent increases in macroalgae related to N enrichment?

## 103 **Methods**

### 104 **Site Description**

105 Moorea, French Polynesia (17° 30'S, 149° 50'W) is a small (~ 135 km<sup>2</sup>) volcanic island  
106 located near the larger island of Tahiti in the central South Pacific. The ocean surrounding

107 Moorea is oligotrophic, with levels of dissolved inorganic nitrogen (DIN) often at or below  
108 detection limits (nitrate plus nitrite in the top 25 m of the water column:  $0.38 \pm 0.84 \mu\text{M}$ ; mean  
109  $\pm$  SD) (Alldredge and Carlson 2019). The island is surrounded by a well-developed barrier reef  
110 located  $\sim 1$  km offshore that is intersected by 12 reef passes that connect the shallow protected  
111 lagoons inside the barrier reef to the open ocean (Fig. 1a). Shoreward of the reef crest is a  
112 distinct back reef habitat that is less than 3 m deep and is dominated by patch reefs separated by  
113 sand, coral rubble, and reef pavement. Directly adjacent to land are shallow fringing reefs that in  
114 some locations are separated from shallow back reef habitats by a channel ( $> 10$  m deep) that  
115 connects to a reef pass.

116 Tidal amplitudes are small ( $< 30$  cm), and circulation within the lagoon is primarily  
117 driven by wave forcing across the reef crest, which creates flow into the lagoon and out of the  
118 reef passes (Hench et al. 2008, Leichter et al. 2013). Wave forcing is largely driven by long  
119 period swells originating from storms thousands of kilometers away. As a result, wave exposure  
120 (and thus circulation patterns) varies seasonally and among sides of the island concurrent with  
121 seasonal differences in storm activity in the northern and southern hemispheres. The west and  
122 east shores receive the most wave energy, with peak wave energy occurring during winter in the  
123 southern hemisphere (hereafter ‘austral winter’) from May to October. In contrast, peak wave  
124 energy on the north shore occurs from November to April during winter in the northern  
125 hemisphere (‘austral summer’) (Edmunds et al. 2010). Moorea’s climate is characterized by a  
126 warm, wet season from November to April and a cooler and drier season from May to October.

127 Due to the steep topography, the island’s  $\sim 17,000$  residents are concentrated along its 60  
128 km coastline, with population centers located in several large valleys. Rapid population increases  
129 in recent decades have coincided with substantial land clearing for agriculture and urbanization

130 (Walker et al. 2014). In contrast to ocean waters, DIN concentrations can be very high (> 100  
131  $\mu\text{M}$ ) in groundwater and streams (Knee et al. 2016, Haßler et al. 2019). Major sources of N to the  
132 lagoons include treated and untreated human sewage, animal waste from livestock, and fertilizer  
133 from agriculture and landscaping (Haßler et al. 2019).

134 **What are the spatial patterns of N enrichment and how do these patterns vary across**  
135 **seasons with different levels of rainfall and wave forcing?**

136 To quantify seasonal variation in nutrient delivery mechanisms, we obtained daily rainfall  
137 and wave data. Rainfall data were from a meteorological station in Faaa, Tahiti (Global  
138 Historical Climatology Network ID:FP000091938), ~ 15 km east of Moorea. We calculated a  
139 30-day moving sum for October 2015 through August 2016, which corresponded with our high  
140 resolution N sampling, and plotted the LOESS smoothed values together with the monthly means  
141 during the different sampling intervals using the R package ggplot2 (Wickham 2016).

142 Wave data have been collected continuously at three sites on the exposed fore reef of  
143 Moorea (one site on each of the island's three sides) since 2005 as part of the MCR LTER  
144 project (<http://mcrlter.msi.ucsb.edu/cgi-bin/showDataset.cgi?docid=knb-lter-mcr.30>; Washburn  
145 2018). At each site, data from bottom-mounted Wave & Tide recorders (SBE 26plus; Sea-Bird  
146 Electronics, Inc., Bellevue, WA, USA) and bottom-mounted Acoustic Doppler Current Profilers  
147 (Sentinel ADCPs: Teledyne RD Instruments, Poway, CA, USA) were used to estimate  
148 significant wave height ( $H_s$ ) and dominant wave period ( $T_p$ ) at 2 h sampling intervals. Daily  
149 averages of  $H_s$  and  $T_p$  were then calculated and total wave power ( $P$ ) per linear meter of reef was  
150 estimated using deep-water approximations as  $P = \rho g^2 H_s^2 T_p / 32 \pi$  where  $\rho$  is seawater density  
151 ( $1025 \text{ kg m}^{-3}$ ) and  $g$  is the acceleration of gravity ( $9.81 \text{ ms}^{-2}$ ).



152 We used ADCPs as the primary instrument to quantify patterns of wave forcing on the  
153 three shores of the island because ADCPs had fewer missing values compared to the SBE 26s  
154 during our study; to obtain a complete record we used data from the SBE 26s when ADCP data  
155 were missing. To ensure that data from the two instruments were comparable, we used the full  
156 time series of wave data in least squares linear regressions to estimate the site-specific log-log  
157 relationships between P as measured by the SBE 26s and ADCPs. The relationships were strong  
158 ( $r^2$  ranging from 0.86 to 0.90), and missing ADCP data were gap filled with the predicted values  
159 based on these site-specific relationships. We then calculated daily mean wave power for each  
160 shore of the island during each 90-day period preceding our sampling efforts. We focused on a  
161 90-day period assuming that N tissue content in the thalli of *Turbinaria ornata* (hereafter,  
162 ‘*Turbinaria*’), the species of macroalgae we used to map N availability, reflects the nutrient  
163 environment during a period of up to three months prior to its collection. This estimate is based  
164 on the growth rates and longevity of *Turbinaria* thalli (Davis 2018, Schmitt et al. 2019).  
165 However, because little is known about N storage and turnover in *Turbinaria* we also describe  
166 rainfall and wave conditions during the 45-day period prior to *Turbinaria* collection (Appendix  
167 S1: Figs. S1 and S2) since these two time scales (45 and 90 days) are likely to bracket the period  
168 of influence.

169 To map N availability in the lagoons of Moorea, we collected samples of *Turbinaria* at ~  
170 180 sites around the island during three different sampling periods, corresponding with different  
171 rainfall and wave regimes (January 2016, May 2016, and August 2016) (Adam and Burkepile  
172 2020). Sites were at least 0.5 km apart and were spaced to maximize coverage of the different  
173 reef habitats within the lagoons, including the fringing reefs, mid-lagoon/back reef, reef crest,  
174 reef passes, and bays (Fig. 1a). Like other macroalgae, *Turbinaria* responds to N pulses by

175 storing surplus N (Schaffelke 1999) and consequently N tissue content is believed to be an  
176 excellent time-integrated indicator of N availability (Atkinson and Smith 1983, Fong et al. 1994,  
177 Shantz et al. 2015). Sampling was conducted over ~ 3 weeks during each of the three sampling  
178 periods; due to logistic constraints, some sites were not sampled in all three sampling periods  
179 (January n = 184, May n = 171, August n = 173). At each of the sites, we collected thalli from 10  
180 different patches of *Turbinaria* across an area of ~ 500 m<sup>2</sup>. Samples were immediately placed on  
181 ice and transported to the laboratory. One blade from each of 10 thalli was sampled at 5 cm  
182 below the apical tip. Blades were scrubbed of epiphytes and rinsed with fresh water before being  
183 dried at 60° C to a constant weight and ground to a fine powder. Total N content was determined  
184 via elemental analysis using a CHN Carlo-Erba elemental analyzer (NA1500) at the University  
185 of Georgia, Center for Applied Isotope Studies.

186           In addition to analyzing N content of algal tissue, we also conducted stable isotope  
187 analyses to help determine the sources of N. The use of naturally occurring stable isotopes of N  
188 (<sup>15</sup>N: <sup>14</sup>N, expressed as δ<sup>15</sup>N) is particularly useful for distinguishing between natural and  
189 sewage-derived N because natural sources generally have low signatures while sewage-derived  
190 N is high in <sup>15</sup>N (with δ<sup>15</sup>N values ranging from ~ 5% to 20%) (Risk et al. 2009, Kendall et al.  
191 2012). In the lagoons of Moorea, N likely comes from a mix of oceanic and terrestrial sources,  
192 the latter including synthetic and organic fertilizers, livestock, and human sewage. Because  
193 synthetic fertilizers tend to have δ<sup>15</sup>N signatures that are similar to or lower than natural sources  
194 (generally ranging from -4 to 4%) (Dailer et al. 2010), elevated δ<sup>15</sup>N values would indicate that  
195 human sewage or animal waste are important sources of N but would not rule out the importance  
196 of fertilizers or other sources. Isotopic analysis on dried and ground algal tissue was conducted  
197 using a Thermo Finnigan Delta-Plus Advantage isotope mass spectrometer with a Costech EAS

198 elemental analyzer at the University of California, Santa Barbara, Marine Science Institute  
199 Analytical Laboratory.

200 Spatial patterns of N enrichment (total N expressed as % of dry weight) were visualized  
201 using ordinary kriging with a spherical variogram model as implemented in the R package  
202 ‘kriging’ (Olmedo 2014). To test whether enrichment patterns were consistent across sample  
203 periods at the scale of individual sites we used linear correlation, with separate correlations  
204 conducted for each side of the island. Finally, we used ANOVA to test whether N levels varied  
205 among our three sample periods. Because of significant spatial autocorrelation among sites, we  
206 analyzed the mean % N on each of the island’s three shores as a conservative test, using data  
207 only from the set of 155 sites that were surveyed in all three sample periods.

208 Visual inspection of N interpolations suggested that spatial patterns of enrichment were  
209 related to wave power (see Results). Therefore, we used the results of the correlation analysis  
210 described in the previous paragraph to test whether temporal consistency depended on variation  
211 in wave forcing. Specifically, we used Pearson’s correlation to test whether the correlation  
212 coefficient describing the temporal correlation in N enrichment (% N) was related to differences  
213 in mean wave power (specific to each shore) across the different sample periods.

214 **To what extent are spatial patterns of nitrogen enrichment related to anthropogenic**  
215 **inputs?**

216 To test whether spatial patterns of N enrichment were associated with anthropogenic N  
217 inputs into the lagoons, we modeled the distribution of N from sewage and agriculture based on  
218 spatially explicit data from the urban planning office of French Polynesia and the Institut de la  
219 Statistique de la Polynésie Française (ISPF). We mapped the relative input of nutrients from

220 agriculture in the lagoon using a three-step procedure. First, for each catchment area ( $n = 119$ ),  
221 we calculated the total farmed area based on data available from the urban planning office of  
222 French Polynesia, and used it as an estimate of “agriculture intensity”. Second, we estimated the  
223 maximum diffusion potential of each catchment ( $MDP_w$ ) using the following formula:

224  $MDP_w = a * A_w + b$  where  $A_w$  is the size of the catchment  $w$  in square km and  $a$  and  $b$  are the  
225 slope ( $a= 0.0022$ ) and intercept ( $b= 15.82$ ) of the linear relationship, obtained from Adjeroud &  
226 Salvat (1996). This approach is consistent with global (Burgers et al. 2014) and local (Brown et  
227 al. 2017) studies highlighting the positive correlation between  $A_w$  and nutrient discharge to the  
228 marine environment, and has been widely used in cumulative impact assessments (Halpern et al.  
229 2008, Ban et al. 2010, Micheli et al. 2013). Third, we applied a kernel density function at each  
230 river mouth that linearly decays “agriculture intensity” of the associated watershed basin from  
231 the river mouth (maximum value) to the  $MDP_w$  (null value) to disperse these watershed-scale  
232 values onto Moorea’s reefs. Then, values were re-scaled from 0 to 1 in order to represent the  
233 relative level of nutrient input from agriculture with the final layer having 5 m resolution. Kernel  
234 estimation was completed using the Heatmap plugin in QGIS v2.18.14 (QGIS Development  
235 Team 2016).

236 We mapped the relative sewage discharge by combining household density along the  
237 coast and the water treatment system used in each individual household ( $n = 8,614$ ). Each  
238 treatment system was assigned a value based on its overall environmental impact (no treatment =  
239 2; treatment with a sump = 1; and treatment with a plant = 0; data from ISPF) which was  
240 subsequently used as a weighting component of household density. We then extrapolated onto  
241 the reef using linear decay, assuming that pollution from sewage discharge spread linearly into

242 the lagoon from the source. Kernel estimation was completed using the Heatmap plugin in QGIS  
243 v2.18.14 (QGIS Development Team 2016).

244 To test whether spatial patterns of N enrichment were related to anthropogenic inputs we  
245 used a two-step approach. First, we tested whether the isotopic signature ( $\delta^{15}\text{N}$ ) of *Turbinaria*  
246 was related to the modeled distributions of N from agriculture and sewage. We found that  $\delta^{15}\text{N}$   
247 signatures were well predicted by modeled sewage input, particularly during the rainy season,  
248 suggesting that  $\delta^{15}\text{N}$  is a good proxy for anthropogenic nutrients (see Results). Thus, to test  
249 whether the overall N enrichment patterns were driven by anthropogenic N input we tested for a  
250 relationship between  $\delta^{15}\text{N}$  and total N. Because we had no a priori expectation of the functional  
251 forms of the relationships between anthropogenic nutrient input, isotopic signature ( $\delta^{15}\text{N}$ ), and  
252 total N, we used boosted regression tree (BRT) analyses; BRTs are a powerful machine learning  
253 approach to model fitting that use the data to characterize the relationships between variables  
254 (Elith et al. 2008, De'Ath and Fabricius 2010). BRT models were conducted using the 'dismo'  
255 package in R (Hijmans et al. 2017) and parameterized according to Elith et al. (2008). Island  
256 shore was included in all models. In addition, to explore whether models had greater prediction  
257 power for some shores compared to others we also created separate models for each island shore.  
258 To aid in data interpretation we show both the fitted relationships from the BRT analyses as well  
259 as correlation plots of the raw data.

## 260 **Are recent increases in macroalgae related to nitrogen enrichment?**

261 To track long-term variation in N availability to benthic organisms, we collected data on  
262 N content of *Turbinaria* tissue annually between 2007 and 2013 as part of the Moorea Coral  
263 Reef Long-Term Ecological Research (MCR LTER) program ([http://mcrlter.msi.ucsb.edu/cgi-](http://mcrlter.msi.ucsb.edu/cgi-bin/showDataset.cgi?docid=knb-lter-mcr.20)  
264 [bin/showDataset.cgi?docid=knb-lter-mcr.20](http://mcrlter.msi.ucsb.edu/cgi-bin/showDataset.cgi?docid=knb-lter-mcr.20); Carpenter 2018). This time frame captures the

265 period when macroalgae increased markedly at some locations in the lagoons. We sampled 10  
266 *Turbinaria* from 18 locations on six cross-shore transects (corresponding to the six core MCR  
267 LTER sites), with samples taken on the fringing reef, back reef, and reef crest during the last  
268 week of May or first week of June. Total N content was determined via CHN analysis on a  
269 model CEC 440HA organic elemental analyzer at the University of California, Santa Barbara,  
270 Marine Science Institute Analytical Laboratory. To determine whether N enrichment varied  
271 consistently among sites, habitats, and years we used ANOVA and AICc to select among models  
272 with and without interaction coefficients (Burnham and Anderson 2002). For this and other  
273 linear models, we inspected model residuals to ensure the assumptions of the tests were met.

274 To characterize the dynamics of macroalgae and coral, we collected data annually in  
275 three habitat types (fringing reef, back reef, and fore reef) at six sites (two on each of the three  
276 sides of the island) from 2006 to 2018 as part of the Moorea Coral Reef Long-Term Ecological  
277 Research (MCR LTER) program ([http://mcr\\_lter.msi.ucsb.edu/cgi-](http://mcr_lter.msi.ucsb.edu/cgi-bin/showDataset.cgi?docid=knb-lter-mcr.8)  
278 [bin/showDataset.cgi?docid=knb-lter-mcr.8](http://mcr_lter.msi.ucsb.edu/cgi-bin/showDataset.cgi?docid=knb-lter-mcr.8); Carpenter 2019). Here we focus on the back reef  
279 habitat, where macroalgae increased in abundance in some locations (Schmitt et al. 2019). At  
280 each site, the dominant space holders are characterized using point contacts at 50 fixed locations  
281 on five permanent 10 m long transects ( $n = 10$ , 0.25 m<sup>2</sup> quadrats per transect). Macroalgae are  
282 identified to species in situ with other benthic space holders categorized to functional group (e.g.,  
283 turf algae, scleractinian coral, etc.). In addition to benthic space holders, annual data on the  
284 abundance and biomass of fishes are collected at the same sites via visual surveys on four 50 m  
285 long by 5 m wide fixed transects ([http://mcr\\_lter.msi.ucsb.edu/cgi-](http://mcr_lter.msi.ucsb.edu/cgi-bin/showDataset.cgi?docid=knb-lter-mcr.6)  
286 [bin/showDataset.cgi?docid=knb-lter-mcr.6](http://mcr_lter.msi.ucsb.edu/cgi-bin/showDataset.cgi?docid=knb-lter-mcr.6); Brooks 2018).

287 To determine whether the persistent increases in macroalgae that occurred on the back  
288 reef were related to spatial patterns of N enrichment and/or herbivore biomass we tested for an  
289 association between the change in the mean percent cover of macroalgae at each of our six long-  
290 term sites and 1) mean N enrichment, and 2) mean biomass of herbivorous fishes during the time  
291 when the coral-to-macroalgae phase shifts occurred (between 2007 and 2013). Ideally, we would  
292 use a model selection framework to disentangle the multiple factors that may be driving  
293 increases in macroalgae. Yet, with only six sites this was not possible. Instead we used two  
294 separate Spearman's rank correlations to independently test for an association between N and  
295 macroalgae and herbivore biomass and macroalgae. A positive correlation between N and  
296 macroalgae would indicate that reefs that have been consistently enriched in N were more likely  
297 to experience increases in macroalgae than less enriched reefs but would not rule out the  
298 importance of other factors. Similarly, a negative correlation between herbivore biomass and  
299 macroalgae would indicate that reefs with the highest biomass of herbivores were least likely to  
300 experience increases in macroalgae.

## 301 **Results**

### 302 **What are the spatial patterns of N enrichment and how do these patterns vary across** 303 **seasons with different levels of rainfall and wave forcing?**

304 Rainfall varied among the three sample periods, reflecting typical seasonal patterns in  
305 Moorea. During 2016, mean monthly rainfall was more than 3-fold greater prior to the May  
306 sampling, compared to the January and August sampling (January = 121 mm, May = 372 mm,  
307 August = 110 mm) due to abundant rainfall during February, March, and April (Fig. 1b).

308 Wave power varied greatly among the three sides of the island and exhibited different  
309 seasonal patterns reflecting differences in exposure to waves generated from storms in the  
310 southern and northern hemispheres (Fig. 1c-e). Wave power was most variable on the north  
311 shore (among period CV = 70%), intermediate on the west shore (among period CV = 40%), and  
312 least variable on the east shore (among period CV = 28%). Mean daily wave power was  
313 consistently high on the north shore prior to the January and May sampling periods but dropped  
314 precipitously in May and remained low throughout the austral winter (Fig. 1c). The result was a  
315 seven-fold decline in wave power on the north shore in the three months leading up to the  
316 August sampling relative to the previous three months. Wave power was consistently high on the  
317 west shore, with wave power exceeding the north shore during all sampling periods (Fig. 1e).  
318 Wave power was especially high on the west shore during the austral winter, with wave power ~  
319 2-fold greater in the three months leading up to the August sampling compared to the three-  
320 month period preceding the January sampling (Fig. 1e). Mean wave power on the east shore was  
321 intermediate between the north and west shores. Similar to the west shore, wave power was  
322 greatest on the east shore during the austral winter and least during the austral summer (Fig. 1d).

323 Nitrogen content of *Turbinaria* tissue revealed evidence for enrichment hotspots on all  
324 three sides of the island (Fig. 2). Algae were enriched in N near bays and large watersheds and  
325 were also frequently enriched near reef passes. In contrast, algae tended to be lower in N near the  
326 reef crest and in the mid-lagoon (Fig. 2). Enrichment patterns varied through time and were  
327 related to seasonal changes in wave power and rainfall. Algae were more enriched in N in May  
328 following the rainy season compared to January and August, which followed drier periods  
329 (ANOVA,  $F_{2,6} = 18.4$ ,  $P = 0.003$ ; Post hoc Tukey tests comparing % N in May to January and  
330 August,  $P < 0.01$  for both). The spatial extent of enrichment appeared to be related to the wave



331 regime. During periods of low wave forcing (e.g., the north shore during August), enrichment  
332 signals were constrained to nearshore fringing reefs and reef passes compared to periods of high  
333 wave forcing (e.g., the west shore during August) when enrichment signals extended farther into  
334 the lagoons (Fig. 2).

335 Enrichment patterns were more consistent throughout the year on some sides of the island  
336 compared to others. Spatial patterns of enrichment were highly consistent on the east shore,  
337 where wave forcing was least variable among seasons (Appendix S1: Fig. S3). In contrast,  
338 enrichment patterns were much more variable on the north shore where wave forcing was highly  
339 variable (Appendix S1: Fig. S4). Spatial patterns of enrichment on the west shore were  
340 intermediate in consistency compared to the other two shores (Appendix S1: Fig. S5). Pairwise  
341 correlation of algal N content among sites during different seasons was strongest when wave  
342 power was similar, as indicated by a negative association between the among-period correlation  
343 coefficient and the difference in mean wave power during the 90-day period immediately  
344 preceding sampling (Pearson's correlation,  $r = -0.59$ ,  $P = 0.09$ ; Appendix S1: Fig. S6).

345 **To what extent are spatial patterns of nitrogen enrichment related to anthropogenic**  
346 **inputs?**

347 Isotopic signature ( $\delta^{15}\text{N}$ ) of *Turbinaria* exhibited strong spatial patterns that varied  
348 considerably among sample periods (Fig. 3b, Appendix S1: Fig. S7). During the rainy season,  
349 when anthropogenic inputs of N are likely to be highest, kernel density estimates of human  
350 sewage derived from data on household sanitation predicted well  $\delta^{15}\text{N}$  values in *Turbinaria* (Fig.  
351 3a-e) (BRT full model cross validation correlation = 0.51; relative importance of modeled  
352 sewage = 75%). The fitted relationship between modeled sewage and  $\delta^{15}\text{N}$  was positive and  
353 roughly linear across most of the range of the data (Appendix S1: Fig. S8).  $\delta^{15}\text{N}$  was also

354 positively related to modeled nutrients from agriculture (Appendix S1: Fig. S8), though  
355 agriculture had little predictive power compared to sewage (BRT relative importance = 7%).  
356 Kernel density estimates of human sewage were also correlated with  $\delta^{15}\text{N}$  during the January and  
357 August sampling (Appendix S1: Figs. S8, S9), though the correlations were less strong (January:  
358 full model cross validation correlation = 0.48; relative importance of modeled sewage = 59%;  
359 August: full model cross validation correlation = 0.38; relative importance of modeled sewage =  
360 30%) and the fitted relationships were highly non-linear with  $\delta^{15}\text{N}$  initially decreasing with  
361 predicted sewage before increasing at higher levels (Appendix S1: Fig. S8).

362 Model performance also varied for different sides of the island. For example, during the  
363 rainy season, modeled sewage predicted as much as 73% of the variation in  $\delta^{15}\text{N}$  on the east  
364 shore of the island (BRT cross validation correlation = 0.73; relative importance of modeled  
365 sewage = 100%). In contrast, modeled sewage during the rainy season only predicted 24% of the  
366 variation in  $\delta^{15}\text{N}$  on the west shore (BRT cross validation correlation = 0.32; relative importance  
367 of modeled sewage = 100%) and 53% of the variation in  $\delta^{15}\text{N}$  on the north shore (BRT cross  
368 validation correlation = 0.55; relative importance of modeled sewage = 97%). Modeled nutrients  
369 from agriculture consistently had little predictive power (BRT relative importance < 10%).

370 Nitrogen tissue content was positively associated with  $\delta^{15}\text{N}$  during all sample periods, but  
371 the relationship was particularly strong (and roughly linear across most of the range of data)  
372 during the rainy season (Fig. 3f-h; Appendix S1: Figs. S10 and S11) (BRT full model cross  
373 validation correlation = 0.61; relative importance of  $\delta^{15}\text{N}$  = 89%). The association between  $\delta^{15}\text{N}$   
374 and total N was strongest for the north and east shores of the island. For example, during the  
375 rainy season,  $\delta^{15}\text{N}$  predicted 75% and 81% of the variation in total N on these shores,  
376 respectively (BRT cross validation correlation north shore = 0.75, east shore = 0.81) while

377 predicting a more modest 35% of the variation in total N on the west shore (BRT cross validation  
378 correlation = 0.35).

### 379 **Are recent increases in macroalgae related to nitrogen enrichment?**

380 Annual sampling of *Turbinaria* from three habitats at our six long-term sites revealed  
381 strong spatial patterns that were consistent through time (model without interactions  
382 outperformed all other models with a delta AICc  $\geq 13$ ). Algal N content varied strongly among  
383 habitats (ANOVA, Habitat:  $F_{2,108} = 23.3$ ,  $P < 0.001$ ) and sites (ANOVA, Site:  $F_{5,108} = 3.2$ ,  $P =$   
384  $0.009$  (Fig. 4). Algae were enriched in N on nearshore fringing reefs, and to a lesser extent the  
385 back reef, relative to the reef crest (Fig. 4a). These differences mirror long-term differences in  
386 water column DIN over the same time period (Appendix S1: Fig. S12). In addition to these  
387 differences among reef habitats, algae also tended to be more enriched in N at the north shore  
388 sites compared to sites on the east and west shores (Fig. 4b).

389 Beginning at or shortly after the onset of our benthic time series in 2007, corals began to  
390 decline and macroalgae began to increase on the back reef at permanent study sites LTER 1,  
391 LTER 2, and LTER 3 (Fig. 5). By 2013 at LTER 1 and LTER 2, and 2014 at LTER 3, the cover  
392 of macroalgae exceeded coral cover (Fig. 5). Since 2014, coral cover at these sites has continued  
393 to decline or stabilize at low ( $< 5\%$ ) levels while the cover of macroalgae has remained high.  
394 Species composition of algal assemblages varies somewhat among sites; dominant taxa include  
395 the brown algae *Turbinaria ornata*, *Sargassum pacificum*, and *Dictyota bartayresiana* as well as  
396 the red alga *Amansia rhodantha* (Fig. 5). Over the same time period, coral cover has remained  
397 high, and macroalgae cover low at permanent study sites LTER 4, LTER 5, and LTER 6, which  
398 experience lower nutrient conditions compared to LTER 1, LTER 2, and LTER 3 (Fig. 5).  
399 Increases in macroalgae were strongly correlated with the long-term nutrient environment, with

400 higher N associated with greater increases in macroalgae (Spearman correlation,  $r_s = 0.94$ ,  $P =$   
401  $0.02$ ; Fig. 6a). In contrast, there was no significant association between increases in macroalgae  
402 and the mean biomass of herbivorous fishes (Spearman correlation,  $r_s = 0.20$ ,  $P = 0.71$ ; Fig. 6b).  
403 Higher N was also associated with coral decline, although the correlation was only marginally  
404 significant (Spearman correlation,  $r_s = -0.77$ ,  $P = 0.10$ ; Appendix S1: Fig. S13).

## 405 **Discussion**

406         Patterns of N enrichment in the lagoons of Moorea were related to several factors,  
407 including rainfall, wave power, and distance from anthropogenic nutrient sources, particularly  
408 sewage. High resolution maps of N enrichment revealed several patterns that were consistent  
409 among the three sample periods. During all sampling periods, algae had higher N on nearshore  
410 fringing reefs compared to the mid-lagoon and reef crest. In addition, algae were consistently  
411 enriched in N near large watersheds, where inputs of N from sewage and agriculture are high.  
412 Our long-term data indicate that areas of the lagoon that are near shore and close to major  
413 watersheds have been consistently enriched in N for at least a decade. During this time, corals  
414 have decreased and macroalgae have increased at back reef locations with high N, while reefs  
415 with lower levels of N have maintained high cover of coral and low cover of macroalgae.  
416 Importantly, these patchy phase shifts to macroalgae have occurred despite island-wide increases  
417 in the biomass of herbivorous fishes. Similar coral-to-macroalgae phase shifts have been  
418 observed on many reefs globally (e.g., Hughes 1994, Graham et al. 2015, Bozec et al. 2019), and  
419 are often associated with reductions in the biomass of herbivorous fishes due to overfishing. Our  
420 observation that nutrient loading, and not herbivory, is strongly associated with phase shifts in  
421 the lagoons of Moorea emphasizes that bottom-up factors, such as nutrient pollution from

422 sewage and agriculture, can also be important drivers of coral-to-macroalgae phase shifts on  
423 tropical reefs.

424 *Influences of rainfall and wave-driven flow on seasonal patterns of nitrogen enrichment*

425         Many of the enrichment patterns we observed in our high-resolution sampling were  
426 consistent among seasons, yet there were also differences that were related to seasonal  
427 differences in wave forcing and rainfall. For example, overall levels of N in *Turbinaria* tissue  
428 were higher in May following the wet summer period compared to January and August which  
429 followed periods with less rainfall. In addition, spatial patterns of enrichment were related to  
430 wave forcing, which varied asynchronously around the island due to seasonal differences in  
431 wave exposure. During periods of low wave energy, enrichment signals were constrained to  
432 nearshore fringing reefs and embayments, while during periods of higher wave energy  
433 enrichment signals extended farther into the lagoons. The precise mechanisms driving these  
434 spatial patterns are unknown but are likely to be related to circulation since waves are the  
435 primary driver of circulation in the lagoons (Hench et al. 2008, Leichter et al. 2013).

436         Irrespective of the precise mechanism, our finding that rainfall and waves can interact to  
437 determine spatial patterns of nutrient enrichment in a lagoonal coral reef system has important  
438 implications. For example, on the north shore of Moorea where the wave climate is highly  
439 seasonal, the rainy season corresponds with a period of high wave energy. Because increased  
440 rainfall results in N enriched conditions in the lagoons and waves appear to be important for  
441 delivering N to the reef crest, the coincidence of the rainy season with a period of large waves  
442 could result in nutrient pulses to wide reaches of the lagoon that otherwise might be restricted to  
443 the fringing reefs when waves are smaller. Given that waves drive circulation patterns on many

444 tropical oceanic islands (Hench et al. 2008), seasonality in wave-driven circulation could be an  
445 important mechanism driving patterns of nutrient enrichment on many coral reefs.

#### 446 *Anthropogenic nitrogen sources*

447         We observed the highest levels of N enrichment near areas with dense human populations  
448 and known nutrient sources, particularly sewage. In addition, isotopic signatures of N in areas of  
449 high enrichment were consistent with terrigenous rather than oceanic sources of N (Lin and Fong  
450 2008, Dailer et al. 2010, Page et al. 2013). While it was not possible for us to quantify the  
451 relative contributions of all the possible N sources to the lagoons, the strong association between  
452 the predicted spatial distribution of human sewage and the  $\delta^{15}\text{N}$  signature in *Turbinaria* tissue  
453 strongly suggests that algae are incorporating sewage-derived N. In addition, the fact that the  
454  $\delta^{15}\text{N}$  signature predicted well total N tissue content suggests that anthropogenic sources of N  
455 (including sewage) are driving spatial patterns of N availability across the lagoons.

456         In contrast to sewage, our model of N enrichment from agricultural fertilizer was not a  
457 good predictor of the isotopic signature or total N content in *Turbinaria* tissue. The lack of an  
458 isotopic signature is unsurprising, given that  $\delta^{15}\text{N}$  values of fertilizers are often similar to natural  
459 sources (Kendall et al. 2012). Our ability to detect an effect of fertilizer on N tissue content also  
460 may have been limited by the assumptions we made when modeling fertilizer input to the  
461 lagoons. A key assumption of our predictive model was that N from fertilizer was delivered to  
462 the lagoons in surface water runoff via one of several dozen streams around the island. In  
463 contrast, we modeled sewage assuming diffusion from the source based on the assumption that  
464 sewage contamination would primarily reach the lagoons via groundwater. While little is known  
465 about the extent of submarine groundwater discharge in Moorea or the relative importance of  
466 groundwater versus surface water runoff for delivering different types of nutrients, recent studies

467 in Moorea suggest that septic waste and animal manure in groundwater are likely an important  
468 source of N to the lagoons (Knee et al. 2016, Haßler et al. 2019). Given the potential importance  
469 of anthropogenic N input for shaping the structure and function of coral reef ecosystems, future  
470 work is needed to better characterize the sources and delivery pathways of anthropogenic N to  
471 the lagoons.

472 *The role of nitrogen enrichment in driving coral-to-algae phase shifts*

473         Patterns of N enrichment have important implications for understanding the dynamics of  
474 benthic algae, which can strongly influence overall ecosystem health. Nutrient enrichment can  
475 allow for the proliferation of algae that are physiologically unable to grow under nutrient poor  
476 conditions. In addition, excess nutrients can also facilitate algae indirectly through the loss of  
477 top-down control if adding nutrients causes algal production to outpace herbivory (Scheffer et al.  
478 2008, Arias-González et al. 2017, Briggs et al. 2018). In this study, we found that several species  
479 of macroalgae have recently increased in abundance on back reef habitats of Moorea, but only  
480 where levels of N are relatively high. Benthic algal blooms have been noted on some nearshore  
481 fringing reefs in Moorea in the past (Payri 1987, Adjeroud and Salvat 1996, Gattuso et al. 1997),  
482 and it had been hypothesized that those blooms could be related to waste water discharge  
483 (Wolanski et al. 1993, Gattuso et al. 1997). Our results support this hypothesis and also suggest  
484 that the impacts of nutrients may extend beyond nearshore fringing reefs to back reef habitats  
485 farther from shore.

486         Several factors in addition to nutrient enrichment could be contributing to the increases in  
487 macroalgae in the lagoons of Moorea. Phase shifts to macroalgae frequently occur following  
488 large coral-killing disturbances that liberate space for the growth of benthic algae, particularly in  
489 systems with low levels of herbivory due to overfishing (Done et al. 1991, Hughes 1994, Graham

490 et al. 2015). The reefs in Moorea experienced two large coral-killing disturbances in the late  
491 2000's, including an outbreak of corallivorous crown-of-thorns seastars (*Acanthaster planci*;  
492 COTS) and a large cyclone that together reduced the cover of living coral to near zero on the fore  
493 reef (Adam et al. 2011, 2014, Kayal et al. 2012). While reefs in the lagoons were much less  
494 impacted by these disturbances, some reefs have experienced a period of protracted coral decline  
495 that appears unrelated to these recent disturbances (Han et al. 2016, Schmitt et al. 2019, this  
496 study). Coral decline on both the fore reef and within the lagoons coincided with an increase in  
497 the biomass of herbivorous fishes (Adam et al. 2011, 2014, Lamy et al. 2015, Han et al. 2016,  
498 Dubois et al. 2019). Yet, unlike the fore reef, where herbivores controlled the proliferation of  
499 algae and corals have rapidly recovered (Holbrook et al. 2016, 2018), many reefs within the  
500 lagoons have become dominated by persistent algal assemblages, despite the presence of a  
501 diverse and abundant herbivore assemblage (Han et al. 2016, Edmunds et al. 2019). Higher  
502 nutrient loading in the lagoons is one possible explanation for why many reefs within the lagoons  
503 have become dominated by macroalgae while macroalgae have remained uncommon on the fore  
504 reef despite increases in herbivore biomass in both habitats. Likewise, differences in nutrient  
505 enrichment among lagoons may help explain why reefs in some lagoons have undergone  
506 persistent phase shifts to macroalgae, while others remain coral dominated despite similar  
507 increases in the biomass of herbivorous fishes.

508         Patterns of N loading may have also influenced the heterogeneous decline in corals  
509 across the lagoons. In addition to the positive correlation between long-term N enrichment and  
510 increase in macroalgae, N enrichment was also related to the loss of coral cover. Part of the  
511 impact of N on corals could be mediated by the rise in macroalgae, as algae can outcompete  
512 juvenile and adult corals (Bulleri et al. 2013, Brown and Carpenter 2014) and inhibit coral



513 recruitment (Kuffner et al. 2006, Mumby et al. 2016, Bulleri et al. 2018). But, excess nutrients  
514 also can directly negatively impact corals by increasing the prevalence and severity of coral  
515 disease (Bruno et al. 2003, Vega Thurber et al. 2014) and by exacerbating coral bleaching and  
516 mortality during thermal stress events (Wiedenmann et al. 2013, Zaneveld et al. 2016, Burkepile  
517 et al. 2019, Donovan et al. 2020). Human sewage may be particularly harmful to corals as it both  
518 delivers excess nutrients as well as pathogenic microbes that cause coral disease and mortality  
519 (Patterson et al. 2002, Sutherland et al. 2010). Nutrients from sewage and other land based  
520 sources of pollution are also commonly associated with toxins, organic carbon, and sediments,  
521 all of which have direct detrimental effects on corals (Fabricius 2005, Wear and Thurber 2015).

## 522 *Conclusion*

523         Spatial patterns of N availability in the lagoons of Moorea, a small oceanic island in the  
524 South Pacific, are shaped by terrigenous inputs even though lagoons are continuously flushed  
525 with oligotrophic ocean water. Long-term data indicate that reefs experiencing the highest levels  
526 of N enrichment have undergone persistent phase shifts to a macroalgae-dominated state despite  
527 the presence of a diverse and abundant herbivore assemblage. These results indicate that  
528 anthropogenic nutrient pollution is likely an important driver of reef degradation in Moorea.  
529 Persistent phase shifts from coral to macroalgae are a problem on many reefs worldwide and are  
530 often associated with declines in the abundance of herbivorous fishes. Our results emphasize that  
531 bottom-up factors can also play an important role in driving these algal phase shifts. Future work  
532 is necessary to better characterize the sources and impacts of anthropogenic nutrients on Moorea,  
533 but sewage from septic systems appears to be an important contributor. Impacts of nonpoint  
534 sources of N are difficult to isolate yet are likely widespread in tropical countries with coral

535 reefs, underscoring the critical importance of managing watersheds to reduce inputs of nutrients  
536 and other land-based pollutants to coral reef ecosystems.

### 537 **Acknowledgements**

538 National Science Foundation grants OCE-1619697 to SJH, DEB, and RJS, OCE-1547952 to  
539 DEB, and OCE-1236905 and OCE-1637396 for the Moorea Coral Reef LTER to RJS, SJH,  
540 RCC, and P Edmunds, as well as an Agence Nationale de la Recherche grant ANR-14-CE03-  
541 0001-01 to JC supported this research. We thank A. Shantz, K. Munsterman, K. Speare, M. Rice,  
542 A. Duran, K. Seydel, J. Verstaen, R. Honeycutt, D. Cook, M. Ladd, V. Moriarty, C. Gottschalk,  
543 J. Curtis, and G. Paradis for field and laboratory assistance, and A. Thompson, M. Donovan and  
544 J. Lecky for assistance with maps. The digital terrain model used in Figs. 1, 2, and 3 was  
545 provided courtesy of Matthias Troyer and was funded through ETH Zurich and the Hacettepe  
546 University Scientific Research Projects Coordination Unit as part of the Moorea IDEA Project.  
547 Research was completed under permits issued by the Territorial Government of French Polynesia  
548 (Délégation à la Recherche) and the Haut-commissariat de la République en Polynésie Française  
549 (DTRT) (Protocole d'Accueil 2015-2017).

### 550 **Authorship Statement**

551 TCA, DEB, SJH, RJS and RCC designed the study and secured funding; TCA, DEB, AJB, and  
552 RCC performed field work; JC, CL, and LT created empirical models of nutrient discharge; LW  
553 oversaw collection and processing of wave data; TCA conducted analyses and wrote the initial  
554 manuscript draft. All authors contributed to manuscript revisions.

### 555 **References**

556 Adam, T. C., A. J. Brooks, S. J. Holbrook, R. J. Schmitt, L. Washburn, and G. Bernardi. 2014.

557 How will coral reef fish communities respond to climate-driven disturbances? Insight from  
558 landscape-scale perturbations. *Oecologia* 176:285–96.

559 Adam, T. C., and D. E. Burkepile. 2020. MCR LTER: Coral Reef: Nitrogen tissue content in  
560 *Turbinaria ornata*: 2016 data in support of Adam et al. submitted to *Ecological*  
561 *Applications*.

562 Adam, T. C., R. J. Schmitt, S. J. Holbrook, A. J. Brooks, P. J. Edmunds, R. C. Carpenter, and G.  
563 Bernardi. 2011. Herbivory, connectivity, and ecosystem resilience: response of a coral reef  
564 to a large-scale perturbation. *PloS ONE* 6:e23717.

565 Adjeroud, M., M. Kayal, C. Iborra-Cantonnet, J. Vercelloni, P. Bosserelle, V. Liao, Y.  
566 Chancerelle, J. Claudet, and L. Penin. 2018. Recovery of coral assemblages despite acute  
567 and recurrent disturbances on a South Central Pacific reef. *Scientific Reports* 8:9680.

568 Adjeroud, M., F. Michonneau, P. J. Edmunds, Y. Chancerelle, T. L. Loma, L. Penin, L. Thibaut,  
569 J. Vidal-Dupiol, B. Salvat, and R. Galzin. 2009. Recurrent disturbances, recovery  
570 trajectories, and resilience of coral assemblages on a South Central Pacific reef. *Coral Reefs*  
571 28:775–780.

572 Adjeroud, M., and B. Salvat. 1996. Spatial patterns in biodiversity of a fringing reef community  
573 along Opunohu Bay, Moorea, French Polynesia. *Bulletin of Marine Science* 59:175–187.

574 Alldredge, A., and C. Carlson. 2019. MCR LTER: Coral Reef: Water Column: Nearshore Water  
575 Profiles, CTD, Primary Production, and Chemistry ongoing since 2005. [knb-lter-mcr.10.36](https://doi.org/10.6073/pasta/6908c811232b1bf27f384bb1c58837a2)  
576 [doi:10.6073/pasta/6908c811232b1bf27f384bb1c58837a2](https://doi.org/10.6073/pasta/6908c811232b1bf27f384bb1c58837a2).

577 Altieri, A. H., and K. B. Gedan. 2015. Climate change and dead zones. *Global Change Biology*

578 21:1395–1406.

579 Anderson, D. M., A. D. Cembella, and G. M. Hallegraeff. 2012. Progress in understanding  
580 harmful algal blooms: paradigm shifts and new technologies for research, monitoring, and  
581 management. *Annual Review of Marine Science* 4:143–176.

582 Arias-González, J. E., T. Fung, R. M. Seymour, J. R. Garza-Pérez, G. Acosta-González, Y. M.  
583 Bozec, and C. R. Johnson. 2017. A coral-algal phase shift in Mesoamerica not driven by  
584 changes in herbivorous fish abundance. *PLoS ONE* 12(4):e0174855.

585 Atkinson, M., and S. Smith. 1983. C: N: P ratios of benthic marine plants. *Limnology and*  
586 *Oceanography* 28:568–574.

587 Ban, N. C., H. M. Alidina, and J. A. Ardron. 2010. Cumulative impact mapping: Advances,  
588 relevance and limitations to marine management and conservation, using Canada’s Pacific  
589 waters as a case study. *Marine Policy* 34:876–886.

590 Boesch, D. 2002. Challenges and opportunities for science in reducing nutrient over-enrichment  
591 of coastal ecosystems. *Estuaries* 25:886–900.

592 Bozec, Y. M., C. Doropoulos, G. Roff, and P. J. Mumby. 2019. Transient grazing and the  
593 dynamics of an unanticipated coral–algal phase shift. *Ecosystems* 22:296–311.

594 Briggs, C. J., T. C. Adam, S. J. Holbrook, and R. J. Schmitt. 2018. Macroalgae size refuge from  
595 herbivory promotes alternative stable states on coral reefs. *Plos One* 13:e0202273.

596 Brocke, H. J., L. Polerecky, D. De Beer, M. Weber, J. Claudet, and M. M. Nugues. 2015.  
597 Organic matter degradation drives benthic cyanobacterial mat abundance on Caribbean  
598 coral reefs. *PLoS ONE* 10(5):e0125445.

599 Brooks, A. 2018. MCR LTER: Coral Reef: Long-term Population and Community Dynamics:  
600 Fishes, ongoing since 2005. knb-lter-mcr.6.56  
601 doi:10.6073/pasta/d71aa19fed4a6fabf2100383fdbba7040.

602 Brown, A. L., and R. C. Carpenter. 2014. Water flow influences the mechanisms and outcomes  
603 of interactions between massive *Porites* and coral reef algae. *Marine Biology* 162:459–468.

604 Brown, C. J., S. D. Jupiter, S. Albert, C. J. Klein, S. Mangubhai, J. M. Maina, P. Mumby, J.  
605 Olley, B. Stewart-Koster, V. Tulloch, and A. Wenger. 2017. Tracing the influence of land-  
606 use change on water quality and coral reefs using a Bayesian model. *Scientific Reports*  
607 7:4740.

608 Bruno, J. F., I. M. Côté, and L. T. Toth. 2019. Climate change, coral loss, and the curious case of  
609 the parrotfish paradigm: why don't marine protected areas improve reef resilience? *Annual*  
610 *Review of Marine Science* 11:307–334.

611 Bruno, J. F., L. E. Petes, C. D. Harvell, and A. Hettinger. 2003. Nutrient enrichment can increase  
612 the severity of coral diseases. *Ecology Letters* 6:1056–1061.

613 Bulleri, F., M. Couraudon-Reále, T. Lison De Loma, and J. Claudet. 2013. Variability in the  
614 effects of macroalgae on the survival and growth of corals: The consumer connection. *PLoS*  
615 *ONE* 8(11):e79712.

616 Bulleri, F., L. Thiault, S. Mills, M. Nugues, E. Eckert, G. Corno, and J. Claudet. 2018. Erect  
617 macroalgae influences epilithic bacterial assemblages and reduce coral recruitment. *Marine*  
618 *Ecology Progress Series* 597:65–77.

619 Burgers, H. E. R., A. M. Schipper, and A. Jan Hendriks. 2014. Size relationships of water

620 discharge in rivers: scaling of discharge with catchment area, main-stem length and  
621 precipitation. *Hydrological Processes* 28:5769–5775.

622 Burkepile, D. E., A. A. Shantz, T. C. Adam, K. S. Munsterman, K. E. Speare, M. C. Ladd, M. M.  
623 Rice, S. McIlroy, J. C. Y. Wong, D. M. Baker, A. J. Brooks, R. J. Schmitt, and S. J.  
624 Holbrook. 2019. Nitrogen identity drives differential impacts of nutrients on coral bleaching  
625 and mortality. *Ecosystems* <https://doi.org/10.1007/s10021-019-00433-2>.

626 Burnham, K. P., and D. R. Anderson. 2002. Model selection and multimodel inference: A  
627 practical information-theoretic approach. 2<sup>nd</sup> Ed. Springer-Verlag, New York.

628 Carpenter, R. 2018. MCR LTER: Coral Reef: Macroalgal CHN, ongoing since 2005. knb-lter-  
629 mcr.20.17 doi:10.6073/pasta/59244d3280854f513fbb07a749c9b6d1.

630 Carpenter, R. 2019. MCR LTER: Coral Reef: Long-term Population and Community Dynamics:  
631 Benthic Algae and Other Community Components, ongoing since 2005. knb-lter-mcr.8.31  
632 doi:10.6073/pasta/37d9c451a908e4a6f8e7ab914b93f44f.

633 Carpenter, R. C., J. M. Hackney, and W. H. Adey. 1991. Measurements of primary productivity  
634 and nitrogenase activity of coral reef algae in a chamber incorporating oscillatory flow.  
635 *Limnology and Oceanography* 36:40–49.

636 Carpenter, S. R., N. F. Caraco, D. L. Correll, R. W. Howarth, A. N. Sharpley, and V. H. Smith.  
637 1998. Nonpoint pollution of surface waters with phosphorus and nitrogen. *Ecological*  
638 *Applications* 8:559–568.

639 D'Angelo, C., and J. Wiedenmann. 2014. Impacts of nutrient enrichment on coral reefs: New  
640 perspectives and implications for coastal management and reef survival. *Current Opinion in*

641 Environmental Sustainability 7:82–93.

642 Dailer, M. L., R. S. Knox, J. E. Smith, M. Napier, and C. M. Smith. 2010. Using  $\delta^{15}\text{N}$  values in  
643 algal tissue to map locations and potential sources of anthropogenic nutrient inputs on the  
644 island of Maui, Hawai'i, USA. *Marine Pollution Bulletin* 60:655–671.

645 Davis, S. L. 2018. Associational refuge facilitates phase shifts to macroalgae in a coral reef  
646 ecosystem. *Ecosphere* 9(5):e02272. 10.1002/ecs2.2272.

647 De'Ath, G., and K. Fabricius. 2010. Water quality as a regional driver of coral biodiversity and  
648 macroalgae on the Great Barrier Reef. *Ecological Applications* 20:840–850.

649 Done, T. J., P. K. Dayton, A. E. Dayton, and R. Steger. 1991. Regional and local variability in  
650 recovery of shallow coral communities: Moorea, French Polynesia and central Great Barrier  
651 Reef. *Coral Reefs* 9:183–192.

652 Donovan, M. K., T. C. Adam, A. A. Shantz, K. E. Speare, K. S. Munsterman, M. M. Rice, R. J.  
653 Schmitt, S. J. Holbrook, and D. E. Burkepile. 2020. Nitrogen pollution interacts with heat  
654 stress to increase coral bleaching across the seascape. *Proceedings of the National Academy*  
655 *of Sciences*:201915395.

656 Dubois, M., D. Gascuel, M. Coll, and J. Claudet. 2019. Recovery Debts Can Be Revealed by  
657 Ecosystem Network-Based Approaches. *Ecosystems* 22:658–676.

658 Duprey, N. N., M. Yasuhara, and D. M. Baker. 2016. Reefs of tomorrow: eutrophication reduces  
659 coral biodiversity in an urbanized seascape. *Global Change Biology* 22:3550–3565.

660 Edmunds, P. J., T. C. Adam, A. C. Baker, S. S. Doo, P. W. Glynn, D. P. Manzello, N. J. Silbiger,  
661 T. B. Smith, and P. Fong. 2019. Why more comparative approaches are required in time-

662 series analyses of coral reef ecosystems. *Marine Ecology Progress Series* 608:297–306.

663 Edmunds, P. J., J. J. Leichter, and M. Adjeroud. 2010. Landscape-scale variation in coral  
664 recruitment in Moorea, French Polynesia. *Marine Ecology Progress Series* 414:75–89.

665 Elith, J., J. R. Leathwick, and T. Hastie. 2008. A working guide to boosted regression trees.  
666 *Journal of Animal Ecology* 77:802–813.

667 Fabricius, K. E. 2005. Effects of terrestrial runoff on the ecology of corals and coral reefs:  
668 review and synthesis. *Marine Pollution Bulletin* 50:125–46.

669 Fong, P., R. M. Donohoe, and J. B. Zedler. 1994. Nutrient concentration in tissue of the  
670 macroalga *Enteromorpha* as a function of nutrient history - An experimental evaluation  
671 using field microcosms. *Marine Ecology Progress Series* 106:273–282.

672 Gattuso, J.-P., C. E. Payri, M. Pichon, B. Delesalle, and M. Frankignoulle. 1997. Primary  
673 production, calcification, and air-sea CO<sub>2</sub> fluxes of a macroalgal-dominated coral reef  
674 community (Moorea, French Polynesia). *Journal of Phycology* 33:729–738.

675 Gobler, C. J., O. M. Doherty, T. K. Hattenrath-Lehmann, A. W. Griffith, Y. Kang, and R. W.  
676 Litaker. 2017. Ocean warming since 1982 has expanded the niche of toxic algal blooms in  
677 the North Atlantic and North Pacific oceans. *Proceedings of the National Academy of*  
678 *Sciences* 114:4975–4980.

679 Graham, N. A. J., S. Jennings, M. A. MacNeil, D. Mouillot, and S. K. Wilson. 2015. Predicting  
680 climate-driven regime shifts versus rebound potential in coral reefs. *Nature* 518:94–97.

681 Halpern, B. S., S. Walbridge, K. A. Selkoe, C. V. Kappel, F. Micheli, C. D'Agrosa, J. F. Bruno,  
682 K. S. Casey, C. Ebert, H. E. Fox, R. Fujita, D. Heinemann, H. S. Lenihan, E. M. P. Madin,



683 M. T. Perry, E. R. Selig, M. Spalding, R. Steneck, and R. Watson. 2008. A global map of  
684 human impact on marine ecosystems. *Science* 319:948–952.

685 Han, X., T. C. Adam, R. J. Schmitt, A. J. Brooks, and S. J. Holbrook. 2016. Response of  
686 herbivore functional groups to sequential perturbations in Moorea, French Polynesia. *Coral*  
687 *Reefs* 35:999–1009.

688 Haßler, K., K. Dähnke, M. Kölling, L. Sichoix, A. L. Nickl, and N. Moosdorf. 2019. Provenance  
689 of nutrients in submarine fresh groundwater discharge on Tahiti and Moorea, French  
690 Polynesia. *Applied Geochemistry* 100:181–189.

691 Hench, J. L., J. J. Leichter, and S. G. Monismith. 2008. Episodic circulation and exchange in a  
692 wave-driven coral reef and lagoon system. *Limnology and Oceanography* 53:2681–2694.

693 Hijmans, R. J., S. Phillips, J. Leathwick, and J. Elith. 2017. *dismo: Species Distribution*  
694 *Modeling*. R package version 1.1-4.

695 Holbrook, S. J., T. C. Adam, P. J. Edmunds, R. J. Schmitt, R. C. Carpenter, A. J. Brooks, H. S.  
696 Lenihan, and C. J. Briggs. 2018. Recruitment drives spatial variation in recovery rates of  
697 resilient coral reefs. *Scientific Reports*:8:7338.

698 Holbrook, S. J., R. J. Schmitt, T. C. Adam, and A. J. Brooks. 2016. Coral reef resilience, tipping  
699 points and the strength of herbivory. *Scientific Reports* 6:35817.

700 Howarth, R. W. 2008. Coastal nitrogen pollution: A review of sources and trends globally and  
701 regionally. *Harmful Algae* 8:14–20.

702 Hughes, T. P. 1994. Catastrophes, phase shifts, and large-scale degradation of a Caribbean coral  
703 reef. *Science* 265:1547–1551.

704 Kayal, M., H. S. Lenihan, A. J. Brooks, S. J. Holbrook, R. J. Schmitt, and B. E. Kendall. 2018.  
705 Predicting coral community recovery using multi-species population dynamics models.  
706 Ecology Letters 21:1790–1799.

707 Kayal, M., J. Vercelloni, T. Lison de Loma, P. Bosserelle, Y. Chancerelle, S. Geoffroy, C.  
708 Stievenart, F. Michonneau, L. Penin, S. Planes, and M. Adjeroud. 2012. Predator crown-of-  
709 thorns starfish (*Acanthaster planci*) outbreak, mass mortality of corals, and cascading  
710 effects on reef fish and benthic communities. PloS one 7:e47363.

711 Kendall, C., E. M. Elliot, and S. D. Wankel. 2012. Tracing anthropogenic inputs of nitrogen to  
712 ecosystems. Pages 375–449 in R. Michener and K. Lajtha, editors. Stable isotopes in  
713 ecology and environmental science. 2<sup>nd</sup> Ed. Blackwell Publishing, Malden, MA.

714 Knee, K. L., E. D. Crook, J. L. Hench, J. J. Leichter, and A. Paytan. 2016. Assessment of  
715 submarine groundwater discharge (SGD) as a source of dissolved radium and nutrients to  
716 Moorea (French Polynesia) coastal waters. Estuaries and Coasts 39:1651–1668.

717 Kuffner, I. B., L. J. Walters, M. A. Becerro, V. J. Paul, R. Ritson-Williams, and K. S. Beach.  
718 2006. Inhibition of coral recruitment by macroalgae and cyanobacteria. Marine Ecology  
719 Progress Series 323:107–117.

720 Lamy, T., P. Legendre, Y. Chancerelle, G. Siu, and J. Claudet. 2015. Understanding the spatio-  
721 temporal response of coral reef fish communities to natural disturbances: Insights from  
722 beta-diversity decomposition. PLoS ONE 10(9):e0138696.

723 Lapointe, B. E. 1997. Nutrient thresholds for bottom-up control of macroalgal blooms on coral  
724 reefs in Jamaica and Southeast Florida. Limnology and Oceanography 42:1119–1131.

725 Lapointe, B. E. 1999. Simultaneous top-down and bottom-up forces control macroalgal blooms  
726 on coral reefs (Reply to the comment by Hughes et al.). *Limnology and Oceanography*  
727 44:1586–1592.

728 Lapointe, B. E., P. J. Barile, M. M. Littler, and D. S. Littler. 2005. Macroalgal blooms on  
729 southeast Florida coral reefs: II. Cross-shelf discrimination of nitrogen sources indicates  
730 widespread assimilation of sewage nitrogen. *Harmful Algae* 4:1106–1122.

731 Lapointe, B. E., R. A. Brewton, L. W. Herren, J. W. Porter, and C. Hu. 2019. Nitrogen  
732 enrichment, altered stoichiometry, and coral reef decline at Looe Key, Florida Keys, USA: a  
733 3-decade study. *Marine Biology* 166,108.

734 Leichter, J. J., A. L. Alldredge, G. Bernardi, A. J. Brooks, C. A. Carlson, R. C. Carpenter, P. J.  
735 Edmunds, M. R. Fewings, K. M. Hanson, J. L. Hench, S. J. Holbrook, C. E. Nelson, R. J.  
736 Schmitt, R. J. Toonen, L. Washburn, and A. S. J. Wyatt. 2013. Biological and physical  
737 interactions on a tropical island coral reef: Transport and retention processes on Moorea,  
738 French Polynesia. *Oceanography* 26:52–63.

739 Lin, D. T., and P. Fong. 2008. Macroalgal bioindicators (growth, tissue N,  $\delta^{15}\text{N}$ ) detect nutrient  
740 enrichment from shrimp farm effluent entering Opunohu Bay, Moorea, French Polynesia.  
741 *Marine Pollution Bulletin* 56:245–249.

742 Loya, Y. 2004. The coral reefs of Eilat-past, present and future: three decades of coral  
743 community structure studies. Pages 1–34 *in* E. Rosenberg and Y. Loya, editors. *Coral*  
744 *Health and Disease*. Springer, Berlin.

745 MacNeil, M. A., C. Mellin, S. Matthews, N. H. Wolff, T. R. McClanahan, M. Devlin, C.  
746 Drovandi, K. Mengersen, and N. A. J. Graham. 2019. Water quality mediates resilience on

747 the Great Barrier Reef. *Nature Ecology and Evolution* 3:620–627.

748 Micheli, F., B. S. Halpern, S. Walbridge, S. Ciriaco, F. Ferretti, S. Frascchetti, R. Lewison, L.  
749 Nykjaer, and A. Rosenberg. 2013. Cumulative human impacts on Mediterranean and Black  
750 Sea marine ecosystems: assessing current pressures and opportunities. *PloS one*  
751 8(12):e79889.

752 Morris, L. A., C. R. Voolstra, K. M. Quigley, D. G. Bourne, and L. K. Bay. 2019. Nutrient  
753 availability and metabolism affect the stability of coral–symbiodiniaceae symbioses. *Trends*  
754 *in Microbiology* 27:678–689.

755 Mumby, P. J., R. S. Steneck, M. Adjeroud, and S. N. Arnold. 2016. High resilience masks  
756 underlying sensitivity to algal phase shifts of Pacific coral reefs. *Oikos* 125:644–655.

757 Naim, O. 1993. Seasonal responses of a fringing reef community to eutrophication (Reunion  
758 Island, Western Indian Ocean). *Marine Ecology Progress Series* 99:137–151.

759 Olmedo, O. E. 2014. kriging: Ordinary Kriging. R package version 1.1. [https://CRAN.R-](https://CRAN.R-project.org/package=kriging)  
760 [project.org/package=kriging](https://CRAN.R-project.org/package=kriging).

761 Page, H. M., A. J. Brooks, M. Kulbicki, R. Galzin, R. J. Miller, D. C. Reed, R. J. Schmitt, S. J.  
762 Holbrook, and C. Koenigs. 2013. Stable isotopes reveal trophic relationships and diet of  
763 consumers in temperate kelp forest and coral reef ecosystems. *Oceanography* 26:180–189.

764 Patterson, K., J. W. Porter, K. B. Ritchie, S. Polson, E. Mueller, E. Peters, D. Santavy, and G.  
765 Smith. 2002. The etiology of white pox, a lethal disease of the Caribbean elkhorn cora,  
766 *Acropora palmata*. *Proceedings of the National Academy of Sciences* 99:8725–8730.

767 Payri, C. E. 1987. Zonation and seasonal variation of the commonest algae on Tiahura Reef

768 (Moorea Island, French Polynesia). *Botanica Marina* 30:141–150.

769 QGIS Development Team. 2016. QGIS Geographic Information System. Open Source  
770 Geospatial Foundation Project. <http://qgis.osgeo.org>.

771 Rice, M. M., R. L. Maher, A. M. S. Correa, H. V. Moeller, N. P. Lemoine, A. A. Shantz, D. E.  
772 Burkepile, and N. J. Silbiger. 2020. Macroborer presence on corals increases with nutrient  
773 input and promotes parrotfish bioerosion. *Coral Reefs*.

774 Risk, M. J., B. E. Lapointe, O. A. Sherwood, and B. J. Bedford. 2009. The use of  $\delta^{15}\text{N}$  in  
775 assessing sewage stress on coral reefs. *Marine Pollution Bulletin* 58:793–802.

776 Schaffelke, B. 1999. Short-term nutrient pulses as tools to assess responses of coral reef  
777 macroalgae to enhanced nutrient availability. *Marine Ecology Progress Series* 182:305–310.

778 Scheffer, M., E. H. van Nes, M. Holmgren, and T. Hughes. 2008. Pulse-driven loss of top-down  
779 control: The critical-rate hypothesis. *Ecosystems* 11:226–237.

780 Schmitt, R. J., S. J. Holbrook, S. L. Davis, A. J. Brooks, and T. C. Adam. 2019. Experimental  
781 support for alternative attractors on coral reefs. *Proceedings of the National Academy of*  
782 *Sciences*:201812412.

783 Shantz, A. A., and D. E. Burkepile. 2014. Context-dependent effects of nutrient loading on the  
784 coral-algal mutualism. *Ecology* 95:1995–2005.

785 Shantz, A. A., M. C. Ladd, E. Schrack, and D. E. Burkepile. 2015. Fish-derived nutrient hotspots  
786 shape coral reef benthic communities. *Ecological Applications* 25:2142–2152.

787 Sinha, E., A. M. Michalak, and V. Balaji. 2017. Eutrophication will increase during the 21st  
788 century as a result of precipitation changes. *Science* 357:405–408.

789 Smith, S. V, W. J. Kimmerer, E. A. Laws, R. E. Brock, and T. W. Walsh. 1981. Kaneohe Bay  
790 sewage diversion experiment : Perspectives on ecosystem responses to nutritional  
791 perturbation. *Pacific Science* 35:279–395.

792 Sutherland, K. P., J. W. Porter, J. W. Turner, B. J. Thomas, E. E. Looney, T. P. Luna, M. K.  
793 Meyers, J. C. Futch, and E. K. Lipp. 2010. Human sewage identified as likely source of  
794 white pox disease of the threatened Caribbean elkhorn coral, *Acropora palmata*.  
795 *Environmental Microbiology* 12:1122–1131.

796 Szmant, A. M. 2002. Nutrient enrichment on coral reefs: is it a major cause of coral reef decline?  
797 *Estuaries* 25:743–766.

798 Umezawa, Y., T. Miyajima, M. Yamamuro, H. Kayanne, and I. Koike. 2002. Fine-scale mapping  
799 of land-derived nitrogen in coral reefs by  $\delta^{15}\text{N}$  in macroalgae. *Limnology and*  
800 *Oceanography* 47:1405–1416.

801 Vega Thurber, R. L., D. E. Burkepille, C. Fuchs, A. A. Shantz, R. McMinds, and J. R. Zaneveld.  
802 2014. Chronic nutrient enrichment increases prevalence and severity of coral disease and  
803 bleaching. *Global Change Biology* 20:544–54.

804 Walker, B. L. E., D. López-Carr, C. Chen, and K. Currier. 2014. Perceptions of environmental  
805 change in Moorea, French Polynesia: the importance of temporal, spatial, and scalar  
806 contexts. *GeoJournal* 79:705–719.

807 Wear, S. L., and R. V. Thurber. 2015. Sewage pollution: Mitigation is key for coral reef  
808 stewardship. *Annals of the New York Academy of Sciences* 1355:15–30.

809 Wickham, H. 2016. *ggplot2: Elegant Graphics for Data Analysis*. Springer-Verlag, New York.

810 Wiedenmann, J., C. D'Angelo, E. G. Smith, A. N. Hunt, F. E. Legiret, A. D. Postle, and E. P.  
811 Achterberg. 2013. Nutrient enrichment can increase the susceptibility of reef corals to  
812 bleaching. *Nature Climate Change* 3:160–164.

813 Wolanski, E., B. Delesalle, V. Dufour, and A. Aubanel. 1993. Modeling the fate of pollutants in  
814 the Tiahura Lagoon, Moorea, French Polynesia. In: 11th Australasian Conference on  
815 Coastal and Ocean Engineering: Coastal Engineering a Partnership with Nature; Preprints  
816 of Papers. Barton, ACT: Institution of Engineers, Australia, 1993: 583-588.

817 Zaneveld, J. R., D. E. Burkepile, A. A. Shantz, C. E. Pritchard, R. McMinds, J. P. Payet, R.  
818 Welsh, A. M. S. Correa, N. P. Lemoine, S. Rosales, C. Fuchs, J. A. Maynard, and R. V.  
819 Thurber. 2016. Overfishing and nutrient pollution interact with temperature to disrupt coral  
820 reefs down to microbial scales. *Nature Communications* 7:11833.

821

## 822 **Figure Legends**

823 Figure 1. (a) Map of Moorea showing the locations of the six MCR LTER sites and the sampling  
824 grid for the high resolution nutrient maps with sample locations colored according to habitat  
825 type. Shallow lagoon habitat is shown in gray. White space within the lagoons represents non-  
826 reef area (e.g., deep water sandy areas). Land is displayed as a digital elevation model with a  
827 hillshade to show ridgelines and valleys. (b) Rainfall from October 2015 until September 2016 in  
828 Faaa, Tahiti ~ 15 km east of Moorea. Blue curve is the LOESS smoothed 30-day sum. Black  
829 lines are monthly means for each of the three 90-day periods preceding the January, May, and  
830 August sampling. Note that we expect the nutrient content of macroalgal tissue (*Turbinaria*  
831 *ornata*) to reflect the nutrient environment during the ~ 3-month period prior to its collection.  
832 Patterns of wave forcing from October 2015 until September 2016 on the (c) north, (d) east, and  
833 (e) west shores of Moorea. Blue lines are daily wave power calculated from ADCPs. Black lines  
834 are daily means for each of the three 90-day periods preceding the January, May, and August  
835 sampling. Note the highly seasonal pattern of wave forcing on the north shore, with minimal  
836 wave forcing during the austral winter (June to September). Also note the different scales on the  
837 y axes.

838 Figure 2. Spatial patterns of nitrogen enrichment (% N) in tissue from the macroalga *Turbinaria*  
839 *ornata* for the (a) January, (b) May, and (c) August sampling. Arrows are proportional to the  
840 mean wave power on each of the three sides of the island during the 90 days preceding each of  
841 the three sampling efforts. Note that the color scale for %N differs among sample periods. Algae  
842 were consistently enriched in N at fringing reef sites and near reef passes compared to sites near  
843 the reef crest. Enrichment is especially strong near large watersheds, most notably the areas



844 around the two large bays on the north shore of the island as well as the smaller bays on the east  
845 and west shores.

846 Figure 3. (a) Modeled N enrichment based on locations of septic systems and sources of  
847 untreated sewage. (b) Empirical patterns of  $\delta^{15}\text{N}$  in *Turbinaria ornata* tissue during the rainy  
848 season. Association between modeled N from sewage and  $\delta^{15}\text{N}$  for the (c) north, (d) east, and (e)  
849 west shores of Moorea during the rainy season. Association between  $\delta^{15}\text{N}$  and nitrogen content  
850 (% N) of *Turbinaria ornata* tissue during the rainy season on the (f) north, (g) east, and (h) west  
851 shores of Moorea.

852 Figure 4. Mean (+/- SE) N content of *Turbinaria ornata* tissue in (a) three habitats (fringing  
853 reef, back reef, and reef crest) and (b) at six long-term MCR LTER sites (two sites on each of the  
854 three sides of the island) between 2007 and 2013. Note that N is consistently enriched at the  
855 fringing reef sites relative to the back reef and reef crest. Also note that LTER sites 1, 2, and 3  
856 tend to be enriched relative to sites 4, 5, and 6.

857 Figure 5. Area plot showing the percent cover of coral and algae at the six MCR LTER back reef  
858 sites (three sites with relatively high nitrogen: LTER 1, LTER 2, and LTER 3 and three sites  
859 with relatively low nitrogen: LTER 4, LTER 5, and LTER 6) from 2007 through 2018. Also  
860 shown is the mean biomass of herbivorous fishes for the same time period. All values are from  
861 annual sampling.

862 Figure 6. Correlation between the change in the percent cover of macroalgae between 2007 and  
863 2013 at each of the six MCR LTER back reef sites and the mean (a) nitrogen content of  
864 *Turbinaria ornata* tissue and (b) biomass of herbivorous fishes during the same time period.

Figure 1

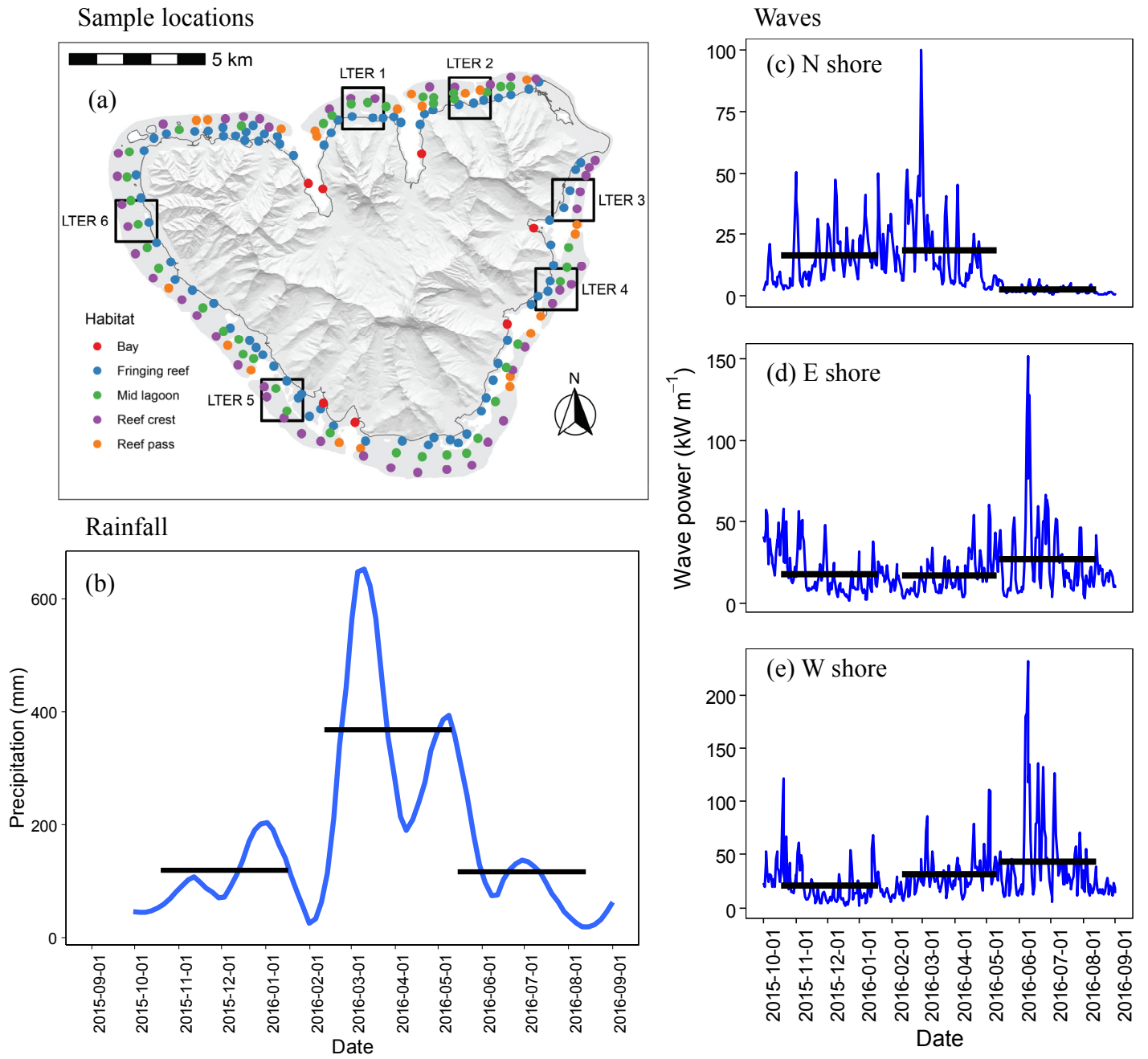
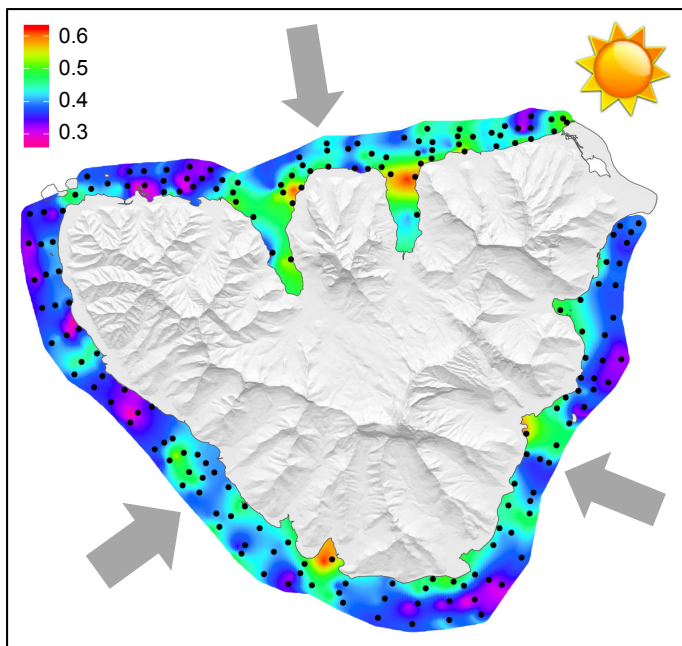
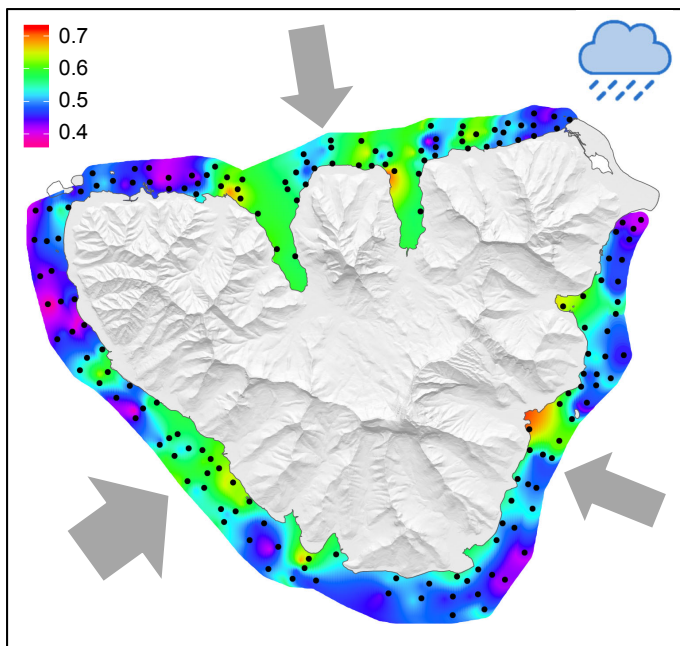


Figure 2

(a) January sampling (dry season)



(b) May sampling (rainy season)



(c) August sampling (dry season)

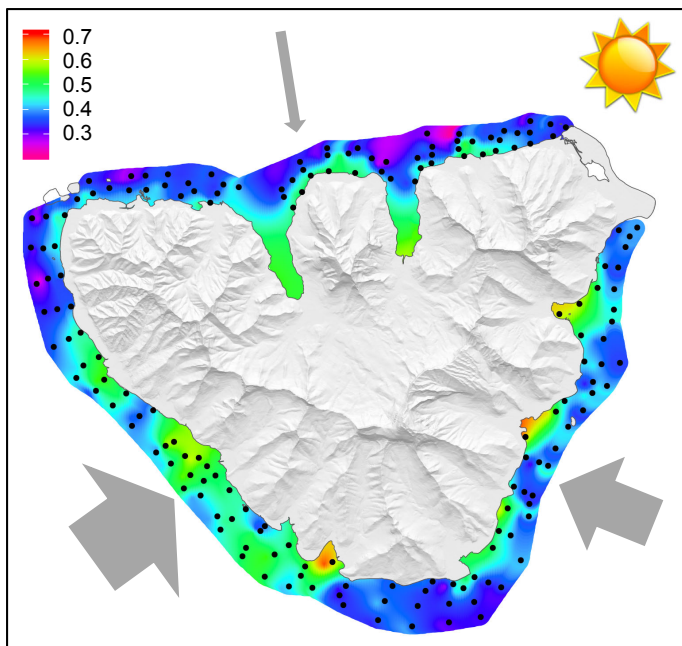
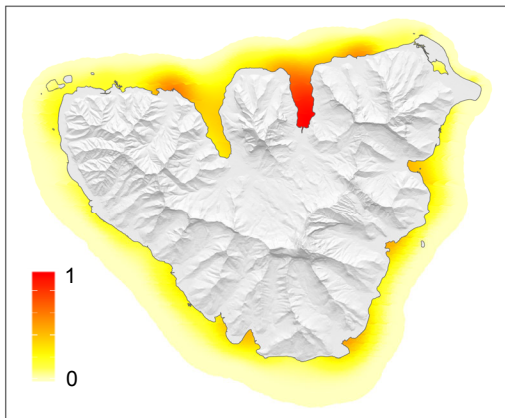


Figure 3

(a) Predicted N from sewage



(b)  $\delta^{15}\text{N}$  during the rainy season

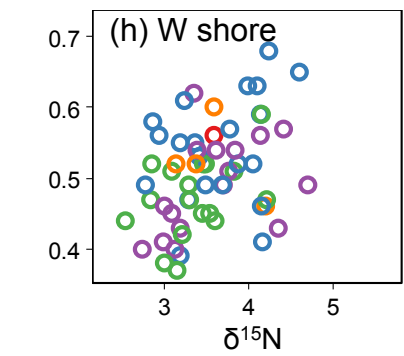
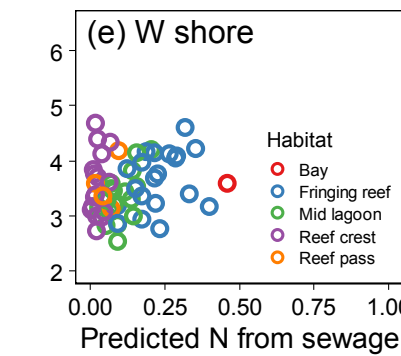
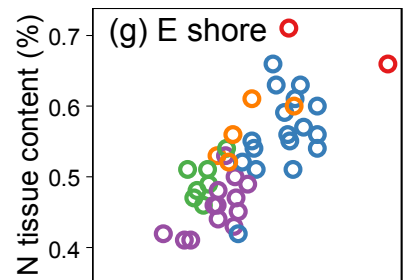
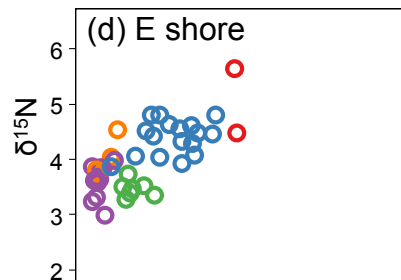
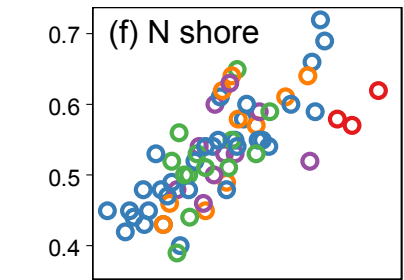
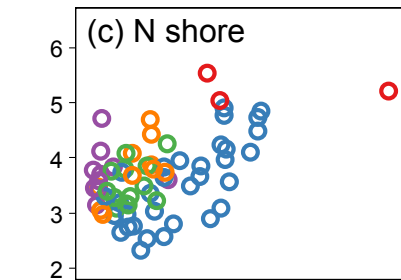
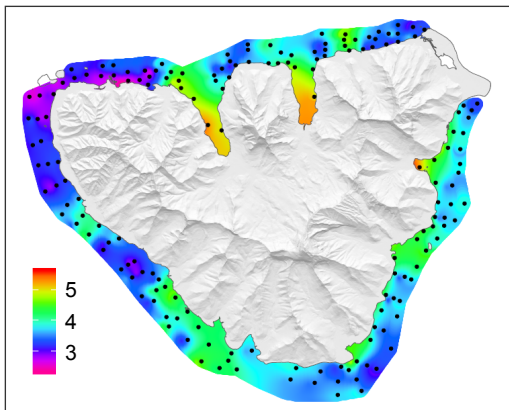


Figure 4

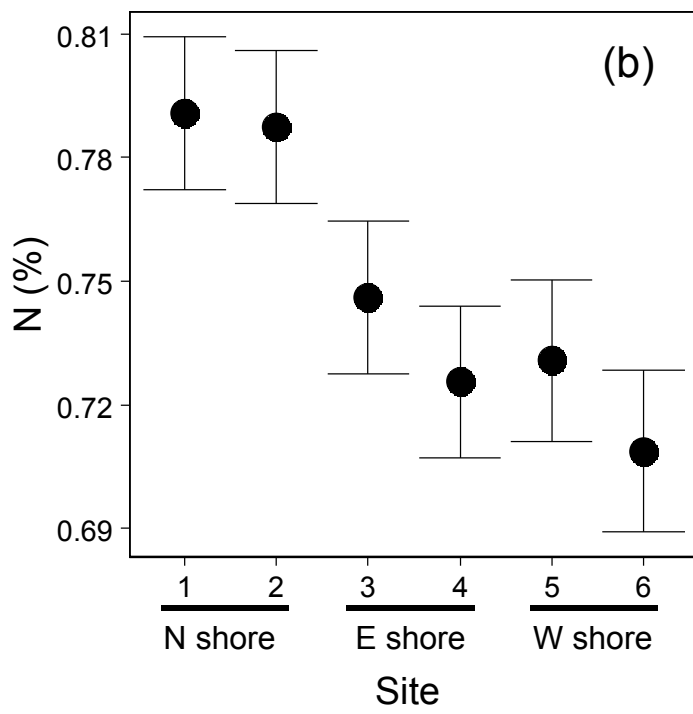
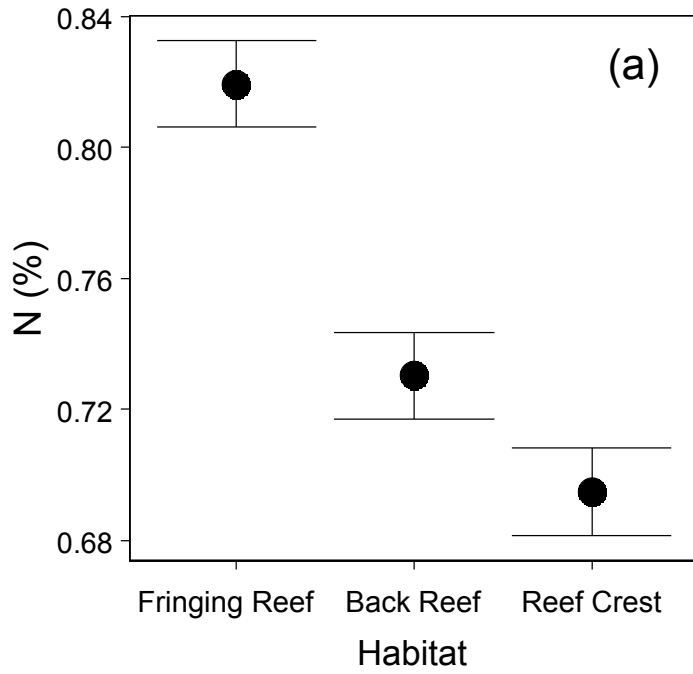


Figure 5

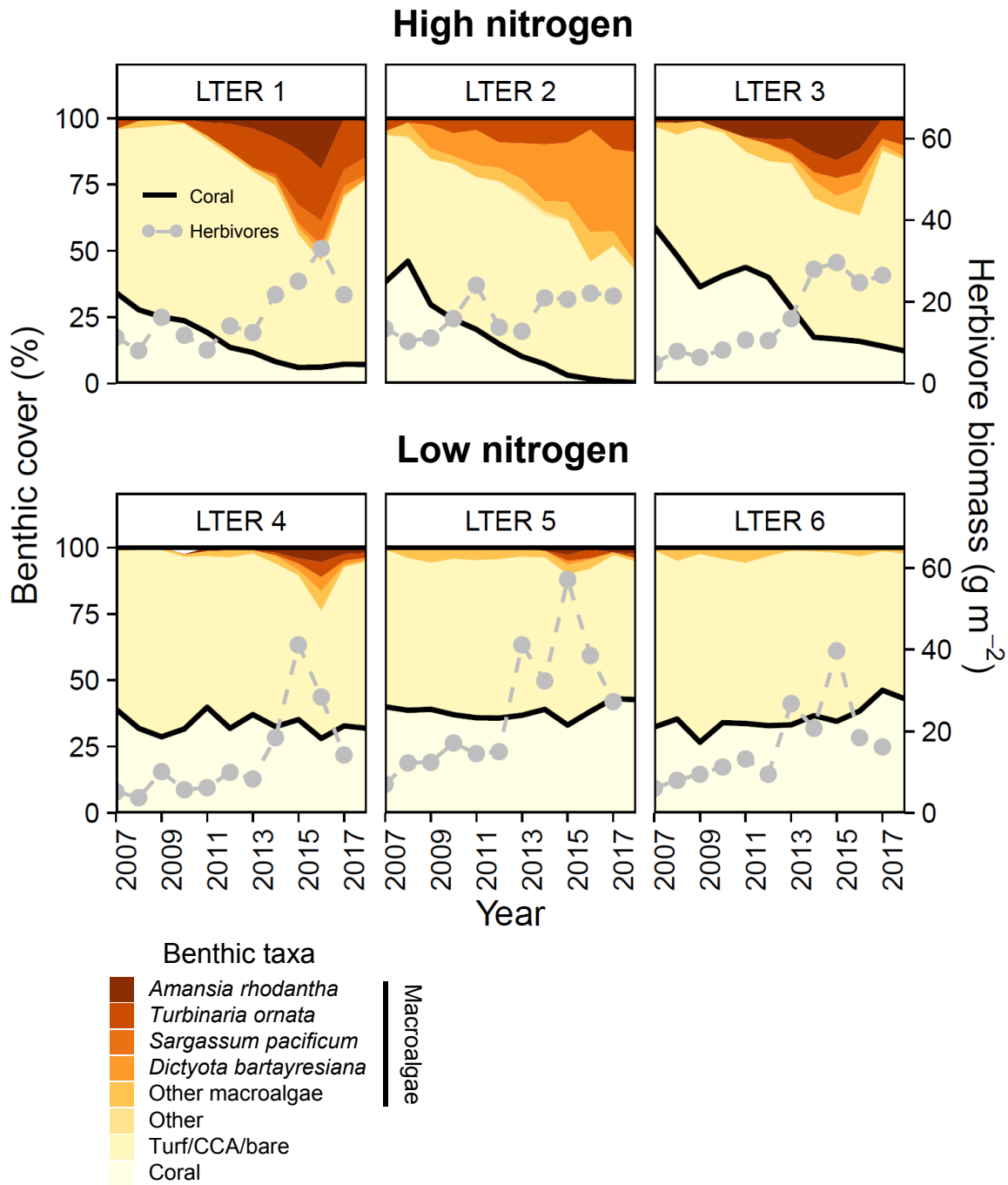


Figure 6

